^{1}H Nuclear Magnetic Resonance Study of the Copper(II)–Carnosine Complex in Aqueous Solution*

M. Ihnat† and R. Bersohn‡

ABSTRACT: The binding of Cu^{2+} to carnosine in deuterium oxide solution was investigated by ^{1}H nuclear magnetic resonance spectroscopy over the pD range 2–12. The interaction was followed by observing the broadening of the carnosine resonances caused by bound Cu^{2+}. At both extremes of pD there is little or no broadening of any resonances. The line breadths of the imidazole protons, $H_{C\text{-}2}$ and $H_{C\text{-}4}$ are equal at all pD's reaching large maxima simultaneously at pD 7.4. The CH band width has a plateau in the region of pD 5–8 whereas two maxima at pD 7.8 and 10.9 are observed for the CH_2(b) band. In alkaline solution, signals of CH_2(a) and CH_2(His) can also be observed. At pD 11.4 equal broadening is observed for the $H_{C\text{-}2}$, $H_{C\text{-}4}$, and CH_2(a) bands, and equal broadening, but smaller by a factor of 20, is observed for the CH, CH_2(b), and CH_2(His) signals. The structures of the complexes were deduced by comparing the observations with relative broadening patterns predicted from molecular models. It is concluded that in acid solution Cu^{2+} is bonded to the carboxylate group of carnosine. In neutral solution the dominant complex involves the N-3 nitrogen of the imidazole ring, whereas at alkaline pD a mixture of the Cu–N-3 complex and one in which the Cu^{2+} is simultaneously bonded to the carboxylate, amino group, and peptide nitrogen exists.

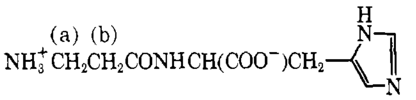
$\mathrm{NH_3^+\overset{(a)}{CH_2}\overset{(b)}{CH_2}CONHCH(COO^-)CH_2}$

The dipeptide carnosine (β-alanyl-L-histidine) is a constituent of muscle and other tissues of vertebrates. Although its biochemical function is so far unknown, an enzyme, carnosinase, which hydrolyzes the peptide bond has been isolated (Hanson and Smith, 1949) and purified (Rosenberg, 1960a). Hanson and Smith observed that the enzyme was stabilized by Mn^{2+} and Zn^{2+}. Rosenberg (1960b, 1961a) found carnosinase to be stabilized by Mn^{2+}, Ca^{2+}, Mg^{2+}, Cd^{2+}, and Zn^{2+}, and activated by Mn^{2+}, Cd^{2+}, Zn^{2+}, and Co^{2+}.

Several proposals have been reported since 1955 for the structure of the Cu^{2+}–carnosine complex in aqueous solution, most based on pH titrations of carnosine with and without Cu^{2+}. Dobbie and Kermack (1955) proposed that above pH *ca.* 5–6, structure **1** represents the complex in which Cu^{2+} is bound to the pyrrole imidazole, amino, and peptide nitrogens, forming two six-membered chelate rings. Martin and Edsall (1960) suggested structure **2** in which the pyridine and not the pyrrole nitrogen of the imidazole is involved in the chelate ring. In order to explain the similarity of the titration curves of Cu^{2+}–carnosine and Cu^{2+}–anserine (β-alanyl-L-1-methylhistidine), Martin (1960) preferred structure **1**. Lenz and Martell (1964) also favored structure **1** for the complex in solution in the region of neutrality and alkaline pH. All these authors agree that in weakly acidic solution Cu^{2+} is bound to the N-1 nitrogen of the imidazole ring, and that as the pH is increased the amino and peptide nitrogens deprotonate and bind to the metal. Lenz and Martell postulated that at low pH, in the early stages of complex formation, the carboxylate group also binds to Cu^{2+} giving a seven-membered chelate ring.

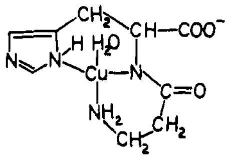

1

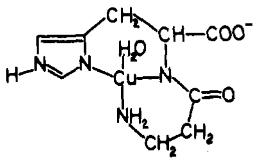

2

Recently, Freeman and Szymanski (1965, 1967) have unequivocally determined, by X-ray crystallography, the structure of the complex in the solid state. Neither **1** nor **2** correctly represents the structure of the alkaline form of the complex. The crystal structure is given in **3**. The complex is a dimer in which the amino nitrogen, peptide nitrogen, and carboxyl oxygen of one peptide molecule, and the 3-nitrogen of the imidazole ring of the second peptide molecule are bonded to Cu^{2+}. The main points of contrast between the structure established for solid state and the structure (**1**)

---

* From the Department of Chemistry, Columbia University, New York, New York 10027. *Received May 15, 1970.* This investigation was supported by the National Institutes of Health Grant CA 07712.

† Present address: Department of Research in Anaesthesia, McIntyre Medical Sciences Building, McGill University, Montreal 110, Quebec, Can.

‡ To whom to address correspondence.

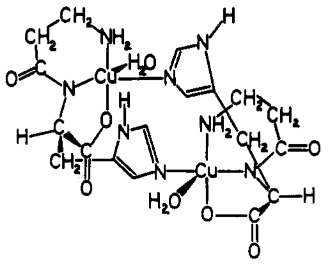

3

proposed for the complex in solution are that the imidazole 3-nitrogen rather than the 1-nitrogen is involved in the solid state, as is the carboxyl group whose involvement in solution was surmized only during the early stages of complex formation, *i.e.*, at low pH.

Much evidence has been amassed regarding the importance of metal ions in many biochemical reactions; the role of copper has recently been discussed (Peisach *et al.*, 1966). The mechanism of catalysis of enzymatic reactions by metal ions by which the metal ions enter the picture either by being an integral part of the enzyme in the case of metalloenzymes or by facilitating binding of the substrate to the enzyme *via* a ternary enzyme–metal–substrate complex has been reviewed (Vallee, 1960; Williams, 1959). Essential to the understanding of such ternary complexes is knowledge of the details of the binding of the metal individually to the enzyme and the substrate. Consequently, by studying the complexation of Cu^{2+} by carnosine, information is being obtained which may be useful in the specific case of the carnosine interaction with carnosinase, and by considering Cu^{2+}–carnosine as a model system for Cu^{2+}–enzyme interactions, data in being gathered which may be helpful in metal–enzyme studies. We report herein, an investigation, by ^1H nuclear magnetic resonance spectroscopy, into the structure of the Cu^{2+}–carnosine complex in aqueous solution over the entire range of pD.

Nuclear Magnetic Resonance. When a paramagnetic metal ion binds to a ligand, it alters both the chemical shifts and band widths of the ligand proton resonances. Overlap of the occupied ligand orbitals with the half-occupied orbitals of the transition metal ion allows the transfer of some electron spin from the metal onto the ligand by a contact hyperfine interaction mechanism, leading to large contact shifts. A dipolar interaction between the electron spin and the proton spin decreases the longitudinal and transverse relaxation times of the proton giving rise to band broadening. Co^{2+} with a short electron spin–lattice relaxation time of *ca.* 10^{-12} sec is an example of a metal whose principle effect is to cause large contact shifts with relatively little broadening, whereas Cu^{2+}, with a much longer electron spin–lattice relaxation time of *ca.* 10^{-8} sec gives rise primarily to band broadening. The interaction of Cu^{2+} with carnosine was investigated by observing broadening of the resonance bands.

The transverse relaxation time in a paramagnetic complex is given by (Carrington and McLachlan, 1967)

$$\frac{1}{T_{2M}} = \frac{1}{15}S(S+1)\left(\frac{g^2\beta^2 g_N{}^2\beta_N{}^2}{\hbar^2 r^6}\right)\left(7\tau_c + \frac{13\tau_c}{1+\omega_s{}^2\tau_c{}^2}\right) + \frac{1}{3}S(S+1)\frac{a^2}{\hbar^2}\left(\tau_e + \frac{\tau_e}{1+\omega_s{}^2\tau_e{}^2}\right) \quad (1)$$

where T_{2M} is the transverse relaxation time of a proton on the coordinated ligand, S is the electron spin, g,β are, respectively, the g value of the electron and Bohr magneton, g_N,β_N are, respectively, the g value of the proton and the nuclear magneton, $\hbar$ is Planck's constant, r is the distance between the proton and metal ion, τ_c is the correlation time for the dipolar interaction between the electron and proton spins, τ_e is the correlation time for contact hyperfine interaction, ω_s is the electron resonance frequency at the field used in observing the nuclear resonance, and a is the isotropic hyperfine splitting constant. For Cu^{2+} the second term in eq 1, the contact term, is usually negligible with respect to the first. Grouping the constants of the first term into one we get

$$\frac{1}{T_{2M}} = \frac{K}{r^6} \quad (2)$$

The observed relaxation time is affected by the rate of exchange of the Cu^{2+} between the complex and the solution. For slow exchange rates, a superposition of two spectra would be observed, sharp bands of the free, uncomplexed ligand, and broad bands of the complex. For the case of rapid exchange, one spectrum, the weighted average of the free and bound ligand, would be observed. On the nuclear magnetic resonance time scale, Cu^{2+} has a rapid exchange rate. We may relate to T_{2M} the observed relaxation time due to Cu^{2+} by

$$\frac{1}{T_{20M}} = \frac{1}{T_{20}} - \frac{1}{T_{2L}} = \frac{1-f}{T_{2L}} - \frac{1}{T_{2L}} + \frac{f}{T_{2M}} \approx \frac{f}{T_{2M}} = \frac{n[Cu^{2+}]}{[L]T_{2M}} \quad (3)$$

where T_{20} is the observed relaxation time, T_{20M} is the observed relaxation time due to Cu^{2+}, T_{2L} is the relaxation time in the free ligand, $f(=n[Cu^{2+}]/[L])$ is the fraction of time the proton spends in the coordination shell of the Cu^{2+}, n is the number of ligands bound to Cu^{2+}, $[Cu^{2+}]$ is the total concentration of Cu^{2+}, and $[L]$ is the total concentration of ligand. The band width at half-height, $\Delta\nu_{1/2}$, is related to the relaxation time by

$$\Delta\nu_{1/2} = \frac{1}{\pi T_2} \quad (4)$$

The observed band-width increment due to Cu^{2+}, $\Delta\nu_{1/2 0 Cu^{2+}}$, in the Cu^{2+}–carnosine case is

$$\Delta\nu_{1/2 0 Cu^{2+}} = \Delta\nu_{1/2 0} - \Delta\nu_{1/2 Car} \quad (5)$$

where $\Delta\nu_{1/2 0}$ is the band width observed in the Cu^{2+}–carnosine solution, and $\Delta\nu_{1/2 Car}$ is that for a pure carnosine solution. Combining eq 2–5 we get

$$\Delta\nu_{1/2 0 Cu^{2+}} = \frac{Kn[Cu^{2+}]}{\pi r^6[Car]} \quad (6)$$

where [Car] is the total carnosine concentration. The band width is thus directly proportional to the Cu^{2+} concentration, and is a sensitive function of r; by observing the effect of Cu^{2+} on various protons of carnosine, it should be possible to locate the Cu^{2+} by triangulation. Similar studies on other systems, making use of the phenomenon of dipolar relaxation have been reported (Li *et al.*, 1962; Sternlicht *et al.*, 1965; Sigel *et al.*, 1969).

Experimental Section

Materials. Carnosine was obtained from Calbiochem and Mann Research Laboratories. The source of Cu^{2+} was Fisher anhydrous $CuCl_2$ dried at 170°. Bio-Rad Laboratories and Columbia Organic Chemicals D_2O was used as solvent. Adjustments of pD were made with 5 M DCl and NaOD prepared from concentrated solutions obtained from Calbiochem and Stohler Isotope Chemicals. Stock solutions of $CuCl_2$ over a wide concentration range were prepared so that convenient, small amounts of the order of 10 mg were required to be added to the carnosine solutions to give desired concentrations of Cu^{2+}. The stock $CuCl_2$ solutions were clarified of a slight turbidity by the addition of very small quantities (*ca.* 1 mg/ml) of 5 M DCl. All solutions were prepared by weighing the components; molarities were calculated taking the density of 0.3 M carnosine to be 1.13 g ml^{-1}. The weights of 5 M DCl or NaOD required to give the desired final pD's were estimated from preliminary experiments. pH was measured at a room temperature of *ca.* 27° with a Sargent combination microelectrode and a Corning pH meter. The silver–silver chloride reference electrode was filled with a saturated solution of potassium chloride in D_2O to minimize the leakage of water into the solution. Conversion into pD units was made according to the equation of Glasoe and Long (1960), pD = pH + 0.40.

Methods. ^{1}H nuclear magnetic resonance spectra were recorded at 60 MHz on a Varian Model A60A spectrometer using precision 5-mm tubes from the Wilmad Glass Co. The temperature of the probe, as determined from methanol and ethylene glycol chemical shifts was 40°. Chemical shifts, δ, of pure carnosine solution were determined relative to DSS[1] (Merck, Sharp and Dohme) used as an internal reference at a concentration of 10^{-2} M. No internal reference was added to solutions containing copper. Band widths[2] measured on spectra usually taken at a sweep width of 100 Hz, a sweep rate of 0.2 Hz sec^{-1}, and a radiofrequency field level of 0.0075–0.010 mG. Spectra substantially broadened by copper were recorded at sweep widths up to 1000 Hz and somewhat higher sweep rates and radiofrequency fields. In all cases care was exercised to prevent distortion by rapid scanning and broadening by saturation. Spectra were usually taken in triplicate. The recorder was calibrated using a mixture of seven reference compounds recommended by Jungnickel (1963). Chemical shifts of the bands in this mixture were obtained at 100 MHz (Varian Model HA100 spectrometer) at a temperature of 31° using a frequency counter, and were converted into 60 MHz and 40°. Agreement with the literature values was within 0.1%. Carnosine shifts were thus corrected; the correction to band widths was negligible and omitted. Spectrometer resolution, as determined by the band width of DSS was usually *ca.* 0.55 Hz. A Dupont 310 curve resolver was used to resolve overlapping resonances.

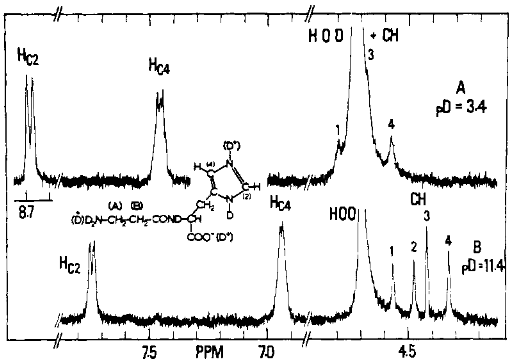

FIGURE 1: ^{1}H resonance spectra of carnosine in D_2O solution–CH and imidazole protons.

Results

Carnosine Chemical Shifts. The ^{1}H nuclear magnetic resonance spectrum of carnosine is sensitive to pD, with changes occurring in the chemical shifts, band widths, and structures of the spin–spin-coupled systems of bands as the pD is raised from acidic to alkaline values. In acid solution (Figures 1A and 2A) the spectrum consists of two low-field resonances at 8.7 and 7.5 ppm downfield from DSS, due to the two carbon-bonded imidazole protons of the histidyl residue, $H_{C\text{-}2}$ and $H_{C\text{-}4}$, respectively, a quartet from the CH at 4.7 ppm, and a complex set of bands in the region 2.6–3.4 ppm arising from the three methylenes. Protons bonded to nitrogen and the carboxyl proton exchange rapidly with the deuterons of the solvent and are not visible. An intense band due to residual HOD is found at a chemical shift of 4.7 ppm, essentially constant over the pD range 2–12. As the pD is increased, the ionizable groups titrate, with neighboring protons suffering upfield shifts due to increased shielding caused by large local decreases in positive charge. In alkaline solution (Figures 1B and 2C) the $H_{C\text{-}2}$ and $H_{C\text{-}4}$ protons have shifted to 7.7 and 6.9 ppm, respectively, the CH quartet is centered at 4.5 ppm, and the three methylene groups now appear at 2.2–3.1 ppm with a clarified spectrum. The spectrum of the methylene region at an intermediate pD is given in Figure 2B. Prolonged storage of alkaline solutions resulted in some exchange of the $H_{C\text{-}2}$ proton for deuterium of the solvent leading to a diminished intensity of the signal.

Assignment of Methylenes. Assignments of the methylene resonances were made by observing the changes in chemical shift as the solution was titrated. The variation with pD of the chemical shifts is presented in Figure 3. Bands G, H, and I (Figure 2) can be followed over the entire pD range, and undergo large changes in shift in alkaline solution in the p*K* region of the amino group. They can thus be assigned to one of the β-alanyl CH_2's. Bands 1–5 (Figure 2B) can be clearly seen at pD $\lesssim$ 10, whereas A, B, C, D, E, and F can be observed at pD $\gtrsim$ 10.5, all bands overlapping at 10 $\lesssim$ pD $\lesssim$ 10.5. The apparent correspondence of curves 1, 2, and 3 in acid solution with their counterparts 1, E, and F in alkaline solution is indicated by dashed portions of the curves. As these bands suffer large changes in chemical shift in the same pD region

---

[1] Abbreviation used is: DSS sodium 2,2-dimethyl-2-silapentane-5-sulfonate.

[2] Chemical shifts are given in parts per million, positive when downfield from DSS: $\delta = (\nu_r - \nu_s)/\nu_0 \times 10^6$, where ν_s and ν_r are the frequencies of the sample and reference bands, respectively, and ν_0 is the operating frequency of 60 MHz.

TABLE I: Effect of Ionization of Amino and Carboxyl Groups on Chemical Shift of Neighboring Methylenes.

Compound	Group	Δδ (ppm)	
		$COOH \rightarrow COO^-$	$NH_3^+ \rightarrow NH_2$
Carnosine	$CH_2(a)$	*a*	0.50
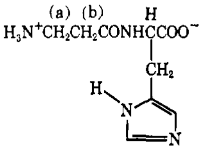	$CH_2(b)$	*a*	0.38^b
γ-Aminobutyric acid	$CH_2(a)$	0.07	0.46
(a) (b) (c)	$CH_2(b)$	0.07	0.25
$H_3N^+CH_2CH_2CH_2COO^-$	$CH_2(c)$	0.25	0.13
β-Alanine	$CH_2(a)$	0.11	0.40
(a) (b)	$CH_2(b)$	0.27	0.26
$H_3N^+CH_2CH_2COO^-$			
Glycyl-L-histidylglycine	$CH_2(a)$	0	0.59^b
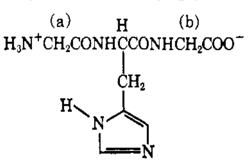	$CH_2(b)$	0.22	0.06^b
Oligoglycines	CH_2 adjacent to NH_3^+	~0	0.51
$H_3N^+(CH_2CONH)_nCH_2COO^-$ $n = 1\text{–}4$	CH_2 adjacent to COO^-	0.26	~0

[a] Not investigated. [b] Changes in δ due to ionization of both imidazole and amino groups.

as G, H, and I, they may also be assigned to one of the β-alanyl methylenes. Since the change in chemical shift, Δδ, of 1, 2(E), and 3(F) is 0.50 ppm, and that of G, H, and I is 0.38 ppm, we assign the former bands to the methylene adjacent to the amino group, CH_2(a), and the latter to the next adjacent amino group CH_2(b).

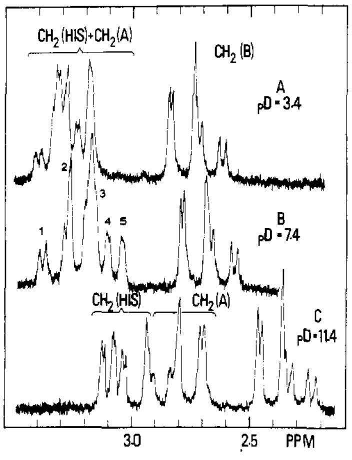

FIGURE 2: ^1H resonance spectra of carnosine in D_2O solution–methylene protons.

To confirm these assignments, chemical shift measurements were made on solutions of the analogous compounds, γ-aminobutyric acid, β-alanine, and glycyl-L-histidylglycine. Table I gives the relevant information. Included are data for the oligoglycines from the work of Nakamura and Jardetzky (1968). The effect of the ionization of the amino group on the chemical shifts of the methylenes gradually decreases with increasing distance from the ionizing group. This is nicely shown by γ-aminobutyric acid and β-alanine. The close agreement of Δδ of the carnosine CH_2(a) with Δδ for the methylenes adjacent to the amino group in γ-aminobutyric acid and β-alanine strengthens the assignment for carnosine. The chemical shift change of carnosine CH_2(b) is somewhat larger than the corresponding Δδ's for the next adjacent methylenes of γ-aminobutyric acid and β-alanine. It is possible that this is due to the additional small effect of the ionization of the imidazole ring, which has been included in the Δδ of 0.38 ppm. In fact, if we again look at Figure 3 and consider the pD range 8.5–12.5, Δδ for G, H, and I becomes *ca.* 0.30 ppm.

Bands 4 and 5 exhibit some chemical shift changes at neutral pD in the region of the p*K* of the imidazole group, and no changes in alkaline solution, leading to their assignment to CH_2(His). Bands A, B, C, and D which can be observed at high pD show no shift changes in the range over which they can be followed, and are consequently also assigned to the

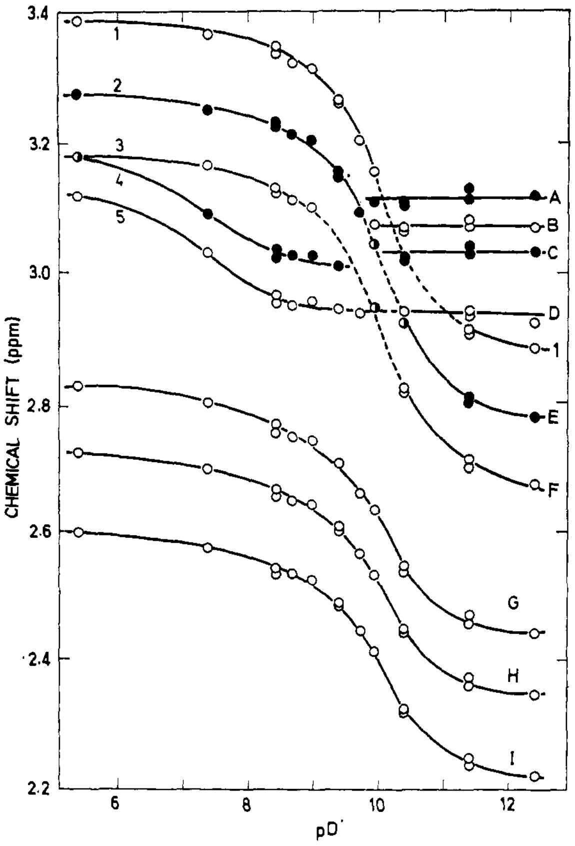

FIGURE 3: Methylene chemical shifts as a function of pD. [carnosine] = 0.31 M. ◑ represents points common to two curves.

histidyl methylene. Curve 5 seems to correspond to curve D. No simple correspondence is observed between curve 4 and A, B, and C. This is not surprising as it has been observed in histidine that the spectrum changes structure and more bands appear as the solution becomes more alkaline. The labeling of the methylene bands in alkaline solution is given in Figure 4.

Estimates of the pK's of the amino and imidazole groups may be deduced from the points of inflection of the curves of Figure 3. The pK (converted from the pK_D scale) of the amino group obtained from 1, 2(E), 3(F), G, H, and I is 9.6; the imidazole pK estimated from 4 and 5 is 7.0. These values are in excellent agreement with average pK's of 9.5 and 6.9 for the amino and imidazole groups, respectively, reported by Dobbie and Kermack (1955), Martin (1960), and Lenz and Martell (1964).

Over the entire range of pD we can clearly observe the resonances of four types of protons, namely, H_{C-2}, H_{C-4}, CH, and CH_2(b), and in alkaline solution also CH_2(a) and CH_2(His). The binding of Cu^{2+} was investigated over the entire pD range by observing the broadening effect on the four proton types visible over the entire range. In alkaline solution use was made of all six proton types.

Carnosine Band Widths. Analysis of the broadening of a single resonance band is inherently simple; analysis of the broadening of a set of partially overlapping spin–spin split bands can be complicated. Carnosine has a moderately complex methylene spectrum even when simplified at high pD.

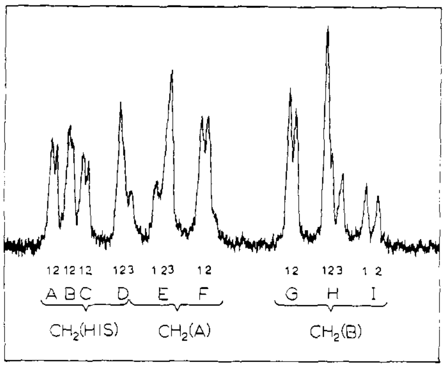

FIGURE 4: Assignment and labeling of the methylene resonances of carnosine at pD 11.4.

Figure 4 shows only three moderately well-separated single bands, and these are of relatively low intensity. All remaining bands are closely spaced doublets or triplets. Bands A, B, C, E, F, G, and H were selected for analysis. A, B, C, F, and G are closely spaced doublets whose components were taken to be equal. E and H are triplets; the largest components, E_3 and H_1 were selected. The H_{C-2} resonance is a symmetrical doublet whereas the H_{C-4} resonance is a closely spaced quintuplet whose structure is clearly evident in acid solution. Component band widths of the former and the overall width of the latter were utilized. The CH quartet, being in the region of the residual HOD band is partially obscured but component 4 could be observed over most of the pD range. In very acidic solutions when component 4 was obscured, component 1 was used instead. Essential characteristics are summarized in Table II and presented in Figure 5.

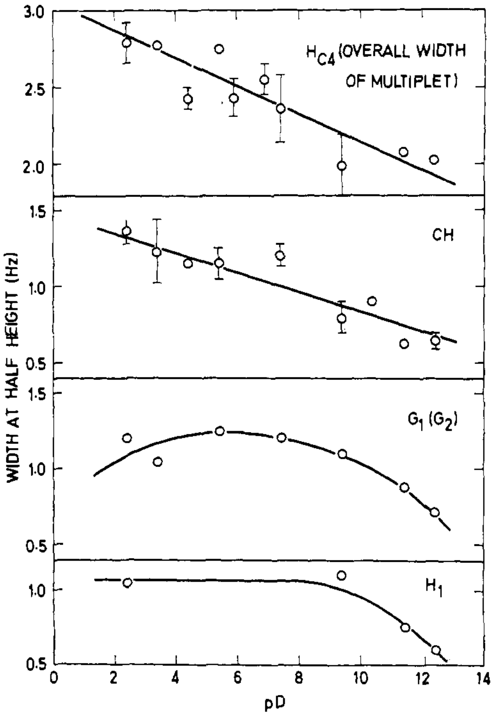

FIGURE 5: Widths of carnosine bands as a function of pD.

TABLE II: Characteristics of Carnosine Band Components.

Band	Separation of Components (Hz)	pD	Band	Width at Half-Height $\Delta\nu_{1/2\,\mathrm{Car}}$ (Hz)[a]	pD
$H_{C\text{-}2}$	1.1–1.4[b]		$H_{C\text{-}2}$	0.77[e]	2–12
$H_{C\text{-}4}$	0.7	*c*	$H_{C\text{-}4}$	*f*	
A	0.8	11.4	CH	*f*	
B	0.6	11.4	A_1,A_2	0.77[g]	11.4
C	0.9	11.4	B_1,B_2	0.83[g]	11.4
$E_{2,3}$	0.8	11.4	C_1,C_2	0.72[g]	11.4
$E_{1,3}$	2.4	11.4	E_3	0.80	11.4
F	1.1	11.4	F_1,F_2	0.90[g]	11.4
G	0.6–1.0[b]		G_1,G_2	*f*	
$H_{1,2}$	1.0	*d*	H_1	*f*	
$H_{1,3}$	2.7	*d*			

[a] Resolution = 0.5 Hz. [b] Function of pD. [c] Acid solution. [d] Determined at pD 11.4, assumed to remain constant in pD range 2–12. [e] Width of components. [f] Function of pD, refer to Figure 5. [g] Mean of both bands.

Band Resolution. Extensive use was made of the Dupont 310 curve resolver in analyzing the spectra. The spectral band components were taken to be Lorentz functions. The sharp bands of unbroadened carnosine spectra could easily be resolved into components. Addition of copper wiped out the fine structure, and much copper (the maximum concentration was *ca.* 10^{-3} M) caused severe broadening and overlap making it impossible to pick out components by direct curve fitting. The technique of curve resolution was then utilized to extract the main bands $H_{C\text{-}2}$, $H_{C\text{-}4}$, CH, A, B, C, E, F, G, and H, and where necessary, resort was made to appropriate graphs of $\Delta\nu_{1/2}$(components) *vs.* $\Delta\nu_{1/2}$(sum of components) to extract estimates of the band widths of the components. Band separations were taken to remain constant in the presence of Cu^{2+}; any possible spin decoupling caused by Cu^{2+} (Kainosho, 1969) was not important because the band widths were linear in added Cu^{2+}.

Carnosine Plus Copper. The characteristics of the Cu^{2+}–carnosine system were studied over the pD range 2–12 with a constant concentration of carnosine (0.31 M) and Cu^{2+} (1.75×10^{-4} M), and in more detail at pD 11.4 and variable Cu^{2+} concentration. The effect of Cu^{2+} on the carnosine spectrum may be demonstrated by referring to Figure 6

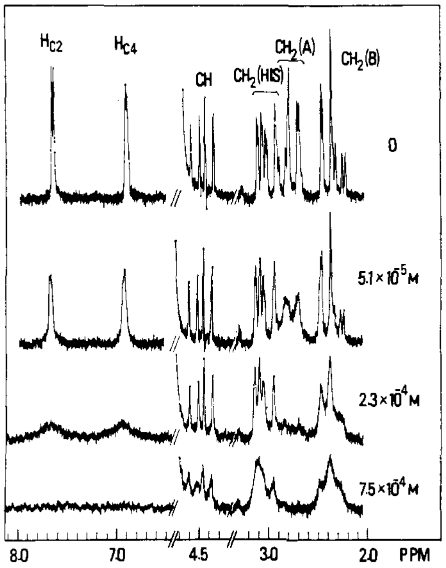

FIGURE 6: Effect of increasing concentration of Cu^{2+} on carnosine resonances. [carnosine] = 0.31 M; pD = 11.4.

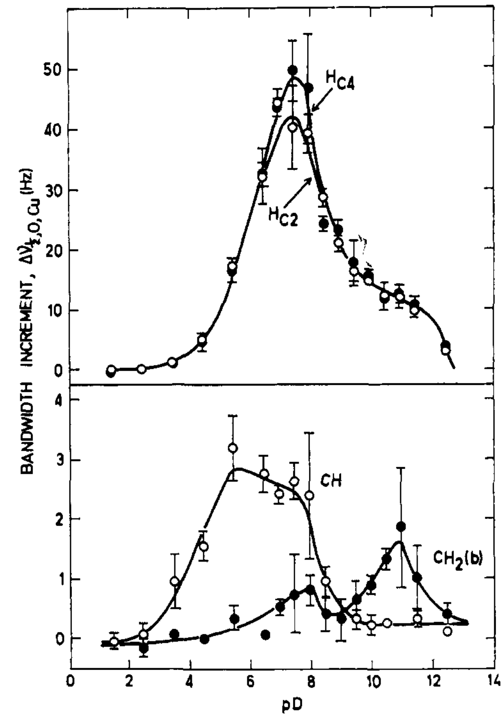

FIGURE 7: Band-width increment due to Cu^{2+} as a function of pD. [carnosine] = 0.31 M; [Cu^{2+}] = 1.75×10^{-4} M. The points for CH_2(b) are averages of values obtained from the G_1(G_2) and H_1 bands.

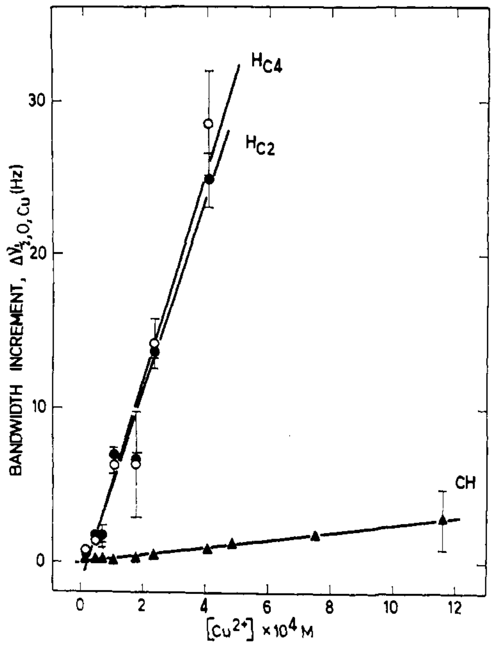

FIGURE 8: Band-width increment due to Cu^{2+} at pD = 11.4. [carnosine] = 0.31 M. (○) H_{C4}, (●) H_{C2}, and (▲)CH.

which shows the spectrum at increasing $[Cu^{2+}]$ at pD 11.4. A dramatic selective effect is shown on the CH_2(a) and imidazole resonances which are the first to be affected at low Cu^{2+} concentrations whereas the CH_2(b), CH_2(His), and CH resonances are unaffected. At higher concentrations, the CH_2(a) and imidazole bands are severely broadened to the point where they are no longer visible, and the CH_2(b), CH_2(His), and CH bands have begun to broaden.

TABLE III: Effect of Cu^{2+} on Carnosine Band Widths at pD 11.4.[a]

Proton	Band	Slope $\frac{d(\Delta\nu_{1/2 0 Cu^{2+}})}{d[Cu^{2+}]}$ ($\times 10^{-4}$ Hz M^{-1})	Mean Slope ($\times 10^{-4}$ Hz M^{-1})	Ratio[b]
H_{C-2}		6.2	6.2	93
H_{C-4}		6.7	6.7	100
CH		0.24	0.24	3.6
CH_2(a)	$F_1(F_2)$	5.9	5.9	88
	E_3	5.9		
CH_2(b)	$G_1(G_2)$	0.37	0.31	4.6
	H_1	0.25		
CH_2(His)	A	0.25	0.28	4.2
	B	0.28		
	C	0.31		

[a] [Carnosine] = 0.31 M; $[Cu^{2+}]$ range = 10^{-5}–1.2×10^{-3} M. [b] H_{C-4} band width taken as 100.

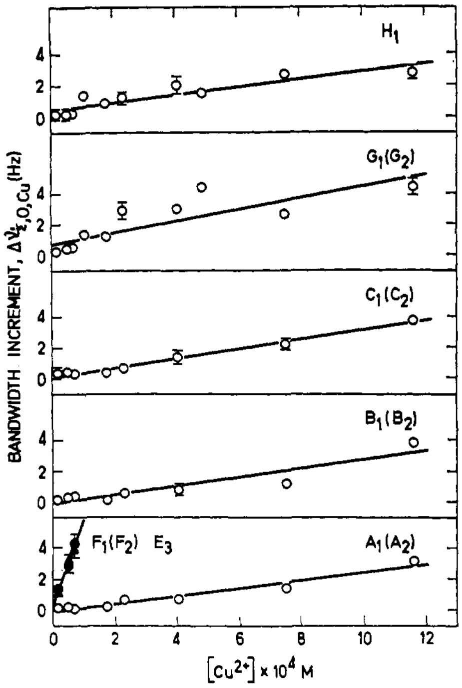

FIGURE 9: Band-width increment due to Cu^{2+} at pD = 11.4. [carnosine] = 0.31 M. (●)$F_1(F_2)$; (▲)E_3. F_1 and E_3 are CH_2(a) bands; A, B, and C belong to the CH_2(His) spectrum; H_1 and G are CH_2(b) bands.

The effect of Cu^{2+} on the band widths of H_{C-2}, H_{C-4}, CH, and CH_2(b) as a function of pD is shown in Figure 7. At both extremes of pD there is little or no broadening of all bands. The imidazole protons both reach large maxima simultaneously at a pD of 7.4 and then fall off more slowly as the pD is increased. The CH band width reaches a plateau in the region 5–8 and then drops to a small value. Two maxima at pD 7.8 and 10.9 are evident for the CH_2(b) curve.

Results of studies in alkaline solution with variable $[Cu^{2+}]$ are presented in Figures 8 and 9 and summarized in Table III. As predicted by eq 6, the plots are linear with the band-width increments proportional to $[Cu^{2+}]$. The largest effect is on the imidazole protons and the terminal methylene, CH_2(a). Much smaller, by a factor of 20, and approximately

TABLE IV: pD for Occurrence of Band-Width Maxima in Cu^{2+}–Carnosine Solutions.[a]

Proton	pD for Maximum Band Width
H_{C-4}	7.5
H_{C-2}	7.3
CH[b]	5.5
	7.5
CH_2(b)	7.8
	10.9

[a] [Carnosine] = 0.31 M; $[Cu^{2+}] = 1.75 \times 10^{-4}$ M. [b] The CH band width has a plateau in the range pD *ca.* 5–8; the two maxima are estimated.

TABLE V: Relative Experimental Band-Width Increments.[a]

pD	Relative Band-Width Increment[b]			
	$H_{C\text{-}2}$	$H_{C\text{-}4}$	CH	CH_2(b)
3	100	100	100	~0
4	100	100	47	~0
5	100	100	23	0.9
6	96	100	13	1.1
7	91	100	6	1.3
7.5	88	100	5	1.7
8	88	100	4.5	2.0
9	100	100	2.5	2.0
10	100	100	1.4	7.2
11	100	100	1.8	15
12	100	100	6.7	20

	$H_{C\text{-}2}$	$H_{C\text{-}4}$	CH	CH_2 (a)	CH_2(b)	CH_2(His)
11.4	100	100	2	104	11	5[c]
	93	100	3.6	88	4.6	4.2[d]

[a] [Carnosine] = 0.31 M; $[Cu^{2+}] = 1.75 \times 10^{-4}$ M. [b] The largest band width is taken as 100. [c] The CH_2(a) and CH_2(His) relative band-width increments are based on averages of values for $[Cu^{2+}] = 1.75 \times 10^{-4}$ M from Figure 9; the others, as all previous band widths are based on data of Figure 7. [d] All band widths were obtained from slopes of band-width increment *vs.* $[Cu^{2+}]$ plots from more intensive investigation at pD 11.4 and are believed to be more accurate; refer to Table III.

equal increments are observed for the CH, CH_2(b), and CH_2(His) bands.

Discussion

The pD's at which the bands have maximum widths are given in Table IV. In comparison to the $H_{C\text{-}2}$, $H_{C\text{-}4}$, and CH_2(b) plots (Figure 7) which have relatively sharp maxima, the CH curve has a broad plateau in the range of pD 5–8. It is tempting to conceive this curve as the sum of two component curves with maxima estimated at 5.5 and 7.5. Relative band-width increments at integral pD's obtained from Figure 7 are presented in Table V. Two sets of data at pD 11.4 are given. For the first set, the data for $H_{C\text{-}2}$, $H_{C\text{-}4}$, CH, and CH_2(b) were obtained from Figure 7, and the data for CH_2(a) and CH_2(His) were obtained from Figure 9. The second set comes from the slopes of band-width increment *vs.* $[Cu^{2+}]$ plots of Figures 8 and 9, and is believed to be more accurate.

The parallel behavior of the $H_{C\text{-}2}$, and $H_{C\text{-}4}$ curves of Figure 7 suggests that the effect arises from the same complex. Furthermore, the virtual superposition of the two curves indicates that the metal ion is equidistant from both imidazole protons and suggests a complex with the Cu^{2+} bound to the N-3 nitrogen of the imidazole ring.[3] Attachment to the N-1 nitrogen would have Cu^{2+} closer to the $H_{C\text{-}2}$ and theoretically the broadening of $H_{C\text{-}2}$ would be greater than $H_{C\text{-}4}$ by a factor of *ca.* 14. The imidazole-bound Cu^{2+} complex exists in varying concentrations over the entire range of pD, reaching a maximum in neutral solution.

Carnosine has five potential binding sites for metal ions: COO^-, NH_2, N(peptide), N-1, and N-3. Possible 1:1 complexes to be considered were established by the use of Corey–Pauling–Koltun atomic models. With no *a priori* knowledge of the types of complexes possible, the number of complexes mathematically possible, in which there are 1–5 ligands bonded to the metal is 31. Of these, the one complex with all five ligands and the five with four ligands cannot be constructed with models and may at once be dropped from further consideration. Of the ten structures with three ligands, three have both N-1 and N-3 simultaneously bonded to Cu^{2+}, an unreasonable structure. Four others could not be constructed leaving three possible structures. Two of these involve bonding to N-1, and in one of these cases the three ligands COO^-, N-1, and N(peptide) are not in a square-planar configuration about Cu^{2+}. As the $H_{C\text{-}2}$ and $H_{C\text{-}4}$ band widths are equal or nearly so, we omit consideration of any complex with N-1 involved. This leaves one tridentate chelate with COO^-, NH_2, and N(peptide) which can easily be constructed, and in which all three ligands are in a square-planar configuration about Cu^{2+}.

Considering now the ten bidentate complexes mathematically possible, the one with simultaneous binding of Cu^{2+} to N-1 and N-3 is again unreasonable. Three, having N-3 as one of the ligands could not be constructed with models and are omitted from consideration as are the three involving N-1. This leaves three possible bidentate complexes.

Bonding of the metal to any one of the five sites is obviously possible. Again we omit the Cu–N-1 complex, and by chemical intuition would not expect to find Cu^{2+} bonded to N(peptide)

---

[3] Recently, Sigel *et al.* (1969), have investigated by ^1H nuclear magnetic resonance spectroscopy, the binding of Cu^{2+} to histidine at pH 7.65, and conclude binding to N-1 of the imidazole ring even though they observe the $H_{C\text{-}2}$ and $H_{C\text{-}4}$ resonances to be equally broadened.

TABLE VI: Properties of Possible Cu^{2+}–Carnosine Complexes.

	Configuration about Cu^{2+a}	No. of Oxygens^b	No. of Nitrogens	Charge
1A	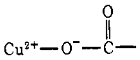 $Cu^{2+}-O^{-}-\overset{\overset{O}{\parallel}}{C}-$	4	0	+3
1B	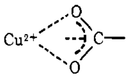	4	0	+3
2	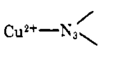	3	1	+2
3	$Cu^{2+}-NH_2-$	3	1	+1
4A	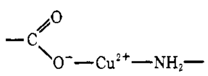	3	1	+1
4B	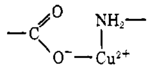	3	1	+1
5	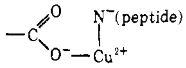	3	1	+1 (0)^c
6	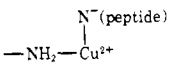 $-NH_2-\overset{\overset{N^{-}(\text{peptide})}{\vert}}{Cu^{2+}}$	2	2	0
7	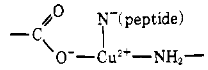	2	2	0
7	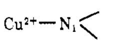	3	1	+2

^{a} D_2O is omitted from these formulas. ^{b} The number of oxygen ligands includes those from D_2O in square-planar configuration about Cu^{2+}. Additional solvent molecules which may occupy the fifth and sixth ligand positions are not considered. ^{c} The charge depends on the state of ionization of the amino group in this hypothetical complex.

alone. We are thus left with seven models of the complexes in solution, the ligands involved being COO^-; NH_2; N-3; COO^-, NH_2; COO^-, N(peptide); NH_2, N(peptide); and COO^-, NH_2, and N(peptide).

Table VI summarizes the complexes considered together with some of their properties. Included is one complex with N-1, only for purposes of comparison. Cu^{2+} may bind to the carboxylate group in two modes indicated by structures 1A and 1B. X-Ray diffraction evidence exists for both types of bonding in complexes of Cu^{2+} with other amino acids. There are also two modes of binding simultaneously to COO^- and NH_2 depicted by 4A and 4B, one in which the two groups make an angle of 180° with each other, the second in which the COO–Cu–NH_2 angle is 90°. Models of all of these complexes were constructed. Various copper–proton distances were obtained by direct measurement and were used to calculate the $(1/r)^6$ broadening factors presented in Tables VII and IX. Within a proportionality constant, $(1/r)^6$ is equal to the bandwidth increment.

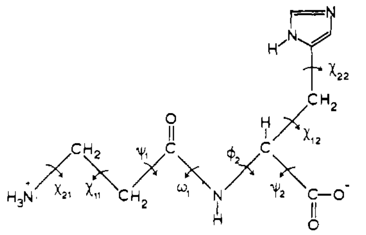

FIGURE 10: Definition of the angles of rotation for carnosine.

The first observation on some of the models was the large variability of the Cu–H distances arising from conformational flexing. In each model, minimum and maximum distances ($r_{\min}$ and $r_{\max}$) of approach of the Cu^{2+} to all of the protons were determined. The extremes of separation are listed in Table VII as $(1/r)^6$. The large variabilities in conformations are evident. In several instances, at closest approach, the copper makes Van der Waals contact with the hydrogen, giving rise to a large broadening factor, whereas when maximally separated, the broadening is diminished by several orders of magnitude. It may be observed that complexes with one ligand, 1A, 2, 3, and 8 have larger variations in $(1/r)^6$ than do those with two or three ligands in which less rotational freedom is possible. Undoubtedly more accurate interatomic distances could be obtained from standard bond lengths and angles, but it was deemed sufficient to rely on models as the major uncertainty is gross conformation.

The conformations of the complexes are functions of eight dihedral angles depicted in Figure 10 indicating rotation about the various bonds of carnosine. The convention regarding the labeling of these angles and choice of zero angle of rotation are essentially those proposed by Edsall *et al.* (1966) with minor changes. When looking down the chain from the amino end toward the carboxylate end, along any bond, the angles are positive for right-handed rotation, *i.e.*, the far end rotates clockwise relative to the near end. The angle χ_{11} is taken to be zero when the C^{β}–N^+H_3 bond is cis to the C^{α}–C' bond for rotation about the C^{α}–C^{β} bond of the β-alanyl chain, and $\psi_1 = 0$ when C^{α}–C^{β} is cis to C'–O for rotation about C^{α}–C'.

Preferred conformations were arrived at from the inspection of models, the guide being attainment of minimum steric hindrance, and magnitudes of the various dihedral angles were estimated visually. The conformation of the peptide group in all structures was assumed to be trans with $\omega_1 = 0$. Rotation about the bonds associated with χ_{21}, ψ_2, and χ_{22} was deemed relatively unimportant in influencing conformation. Consequently these angles were not considered. When possible (structures 1A, 1B, 2, 3, 8), the β-alanyl chain was made fully extended ($\chi_{11} = 180°$, $\psi_1 = 0°$). Dihedral angles in preferred conformations of Cu^{2+}–carnosine complexes are listed in Table VIII. While these values are estimates, they nevertheless indicate the approximate conformational states. A range of values, or more than one value is given for ϕ_2 and χ_{12} as, by inspection of models, no particular value could unequivocally be chosen for the most stable conformer. The spin–spin coupling constants deduced from the splitting of the C–H peak are consistent with χ_{12} values near 180 or 240°. For complex 4A two sets of angles are listed, corre-

TABLE VII: Limits of $(1/r)^6$ Calculated from Cu^{2+}–Proton Distances Measured on Molecular Models.

	$(1/r)_{max}^6$ and $(1/r)_{min}^6 \times 10^6$ (Å^{-6})											
	$H_{C\text{-}2}$											
Complex	Max	Min	$H_{C\text{-}4}$		CH		CH_2(a)		CH_2(b)		CH_2(His)	
1A	460	2.2	3300[a]	4.5	5300[a]	51	3300[a]	2.2	650	5.2	3300[a]	64
1B	22	1.7	390	8.5	140	140	51	1.9	22	3.3	140	26
2	770	770	770	770	51	5.2	330	0.75	51	1.1	33	24
3	240	0.34	5300[a]	0.79	2100	2.9	1700	650	5300[a]	110	5300[a]	1.8
4A	15	5.2	240	22	460	460	650	650	390	390	64	64
4B	5.7	5.7	57	18	140	140	460	460	650	650	460	460
5	140	18	5300[a]	22	460	460	4100[a]	64	2100	240	460	140
6	140	4.5	4100[a]	10	2600	290	770	770	330	330	5300[a]	140
7	64	2.9	3300[a]	15	330	330	770	770	330	330	240	110
8	770	770	57	57	5300[a]	40	4100[a]	1.6	930	5.7	930	180

[a] The Cu^{2+} makes, or almost makes Van der Waals contact with the hydrogen.

sponding to two conformations. $(1/r)^6$ for preferred conformations are listed in Table IX. Large variations in most angles are possible giving rise to the extremes of $(1/r)^6$ listed in Table VII. The next step is to compare the properties of the model compounds with the experimental data to ascertain which structures best explain the observations.

The maxima at pD 7.5 of the $H_{C\text{-}2}$, $H_{C\text{-}4}$, CH, and CH_2(b) band widths suggests one complex reaching a maximum concentration at that pD. At pD 7.5, Table V gives the band-width ratios $H_{C\text{-}2}$:$H_{C\text{-}4}$:CH:CH_2(b) as 88:100:5:1.7. With reference to Table IX only one model, 2, with copper bonded to N-3, has band-width ratios anywhere close to the observed ratios: $H_{C\text{-}2}$:$H_{C\text{-}4}$:CH:CH_2(b) = 100:100:3.1:0.1. Model 2 thus best represents the dominant complex in solution at neutral pD. Persistant $H_{C\text{-}2}$ and $H_{C\text{-}4}$ broadening in acid and alkaline solution implies the existence of complex 2 over the entire range of pD. Only two other complexes, 1A and 1B, have substantially broadened $H_{C\text{-}2}$ and $H_{C\text{-}4}$ resonances. Their preferred conformations (Table IX), however, do not give rise to equal effects on both imidazole protons. Reference to Table VII indicates that due to large possible conformational variations, conformations in which copper is equidistant from the two imidazole protons are conceivable. That these would be the preferred conformations, however, is unlikely, and complex 2 is favored.

TABLE VIII: Dihedral Angles in Preferred Conformations of Cu^{2+}–Carnosine Complexes.

Complex	Dihedral Angle[a] (deg)			
	χ_{11}	ψ_1	ϕ_2	χ_{12}
1A	180	0	0–120, 240	180–240
1B	180	0	0–120, 240	180–240
2	180	0	0–120, 240	180–240
3	180	0	0–120, 240	180–240
4A[b]	60	60	60	180–240
	300	120	60	180–240
4B	60	90	60, 240	180–240
5	180	0	0	60, 240
6	80	140	0–120, 240	180–240
7	120	140	0	230
8	180	0	0–120, 240	180–240

[a] $\omega_1 = 0$ in all structures; χ_{21}, ψ_2, and χ_{22} were not measured. [b] Two sets of angles are given, corresponding to two conformations.

At acid pD the larger CH broadening with respect to $H_{C\text{-}2}$ and $H_{C\text{-}4}$, $H_{C\text{-}2}$:$H_{C\text{-}4}$:CH = 100:100:100 at pD 3, cannot be explained by complex 2. Also the first maximum at pD 5.5 of the CH plot suggests the presence of another complex. The relative band widths of the CH and CH_2(b) protons provide a clue to its identity. Only models 1A and 1B have CH:CH_2(b) ratios in the correct range. Thus at low pD the complex Cu–OOC exists in addition to Cu–N-3, and may be the dominant one. Such a complex is chemically logical as the carboxyl group with a p*K* of 2.6 is the first to ionize and provide an electrostatically attractive ligand for the metal ion. It is not possible to differentiate between complex 1A or 1B.

As the pD is raised to alkaline values, the CH_2(b) curve passes through a second maximum at pD 10.9 suggesting the presence of a third complex. There is a hint of a maximum also for the CH curve but experimental error precludes any such presumption at present. The decrease of all curves in strongly alkaline solution is apparently not due to precipitation of the complex or $Cu(OH)_2$ as a solution 0.1 M in carnosine and 0.05 M in Cu^{2+} at pD 13.5 contained no precipitate. Cu^{2+} still must be complexed by carnosine at this pD as the low-solubility product of $Cu(OH)_2$ precludes the existence of all of the Cu^{2+} in 0.05 M or even 1.75×10^{-4} M Cu^{2+} in the form of soluble $Cu(OH)_2$ (the Cu^{2+} in a 10^{-4} M Cu^{2+} solution will precipitate above pD *ca.* 7). Furthermore, the persistence of an intensely blue color of the Cu^{2+}–carnosine solution indicates presence of a Cu^{2+}–carnosine complex.

TABLE IX: Average Conformation of Complexes $(1/r)^6$ from Preferred Model Conformations.

Complex	H_{C-2} $(1/r)^6$	H_{C-2} Ratio[a]	H_{C-4} $(1/r)^6$	H_{C-4} Ratio	CH $(1/r)^6$	CH Ratio	CH_2(a) $(1/r)^6$	CH_2(a) Ratio	CH_2(b) $(1/r)^6$	CH_2(b) Ratio	CH_2(His) $(1/r)^6$	CH_2(His) Ratio
1A	10	2.2	5.2	1.1	460	100	26	5.7	33	7.2	26	5.7
1B	16	31	45	88	51	100	3.3	6.5	10	20	51	100
2	770	100	770	100	24	3.1	0.72	0.09	0.85	0.11	24	3.1
3	0.34	0.04	0.41	0.04	3.8	0.41	930	100	110	12	1.8	0.19
4A	2.6	0.40	18	2.8	460	71	650	100	390	60	64	9.9
4B	2.3	0.35	15	2.3	140	22	460	71	650	100	460	71
5	4.5	0.21	22	1.1	930	44	64	3.0	2100	100	180	8.6
6	3.8	0.49	26	3.4	650	84	770	100	330	43	240	31
7	3.3	0.43	24	3.1	330	43	770	100	330	43	240	31
8	770	100	57	7.4	330	43	4.8	0.62	20	2.6	290	38

All values: $(1/r)^6 \times 10^6$ (Å^{-6}) and Ratio.

[a] The largest value of $(1/r)^6$ in each set is taken as 100.

It may be speculated that hydroxide may be involved in complexation at very high pD and that insertion of hydroxide between Cu^{2+} and carnosine in the complex would increase the distance between Cu^{2+} and the carnosine protons leading to diminished broadening at very high pD. This point was not pursued further and it was assumed that at pD 11.4 the story is not yet complicated by the existence of hydroxy complexes. The detailed study at pD 11.4 was relied upon to provide information on the nature of the complexes in alkaline solution. The second set of relative band widths at pD 11.4 in Table V is chosen for discussion.

The striking observation about the relative band-width data at pD 11.4 is that the resonances of H_{C-2}, H_{C-4}, and CH_2(a) are all broadened to the same extent, while the CH, CH_2(b), and CH_2(His) bands are also equally affected but to a lesser extent. No model considered has H_{C-2}, H_{C-4}, and CH_2(a) equally broad, so we consider a mixture of two complexes, Cu–N-3 (2), and another complex, the H_{C-2} and H_{C-4} broadening arising from Cu–N-3, the broadening of the remaining protons being due to the second complex. At this pD the concentration of Cu–N-3 is down to about one-fourth of the concentration at pD 7.5. Let us now discuss the CH, CH_2(a), CH_2(b), and CH_2(His) bands.

Considering first the equality of CH, CH_2(b), and CH_2(His) widths, the model which comes closest to approximating this is 7, with model 6 close behind. All other models have larger differences among these band widths. In model 7, the CH and CH_2(b) increments are somewhat larger than that of CH_2(His), whereas experimentally the CH_2(b) band width is slightly larger than the CH and CH_2(His) band widths. Nevertheless, the relative model broadening factors are in remarkably good agreement with the experimental ones. Considering now the 20-fold larger increment of CH_2(a), only model 3 approximately satisfies this requirement. Models 4A, 6, and 7 also have larger CH_2(a) widths but not by a factor of 20. Models with two ligands to copper are favored over model 3 which has only the amino group attached to the metal. All three are similar and we argue in favor of model 7 which should have an edge in stability over the other two due to the presence of a five- and a six-membered chelate ring.

The CH_2(a) band width, as those of other methylenes calculated from models, is based on a mean interatomic distance between Cu^{2+} and the two protons. One of the protons of the CH_2(a) group in complex 7 almost makes Van der Waals contact with Cu^{2+}. It is possible that there may be some overlap of the copper electron wave function with the proton, making the hyperfine constant, a, in eq 1 significant. Consequently it is conceivable that such proximity leads to larger broadening than predicted by the inverse sixth power equation.

The distribution of complexes with pD is summarized in Figure 11. It would be informative if a plot of concentration or fraction of Cu^{2+} present in each species *vs.* pD were presented. The nature of the data, however, precludes such quantitation. In the region of neutrality it appears that Cu–N-3 is the dominant species. If it is assumed to be the sole species, we can make an estimate of the constant K in eq 6. Taking the mean band-width increment for the H_{C-2} and H_{C-4} protons to be 45 Hz, and the Cu–H distances 3.3 Å, we get $K = 3 \times 10^{-40}$ Hz cm^6. Knowing K, one can in principle calculate metal–proton distances from band width determinations on more complicated systems with coordinated Cu^{2+}, and make an estimate of the conformation of the complex. Future publications will touch on this topic.

The three species concluded for the aqueous Cu^{2+}–carnosine system should be looked upon as the major constituents. The existence of minor components is difficult to establish. It may be considered that the formation of the tridentate complex in alkaline solution is a stepwise process so that intermediate bidentate and monodentate species are not out of the question. Only monomer species have been considered as the present technique does not give evidence of dimers and higher aggregates. Recently, Boas *et al.* (1969) have obtained evidence that the copper–carnosine complex is monomeric in aqueous solution.

This investigation is in agreement with previous studies of Cu^{2+}–carnosine in solution in the sense that in acidic

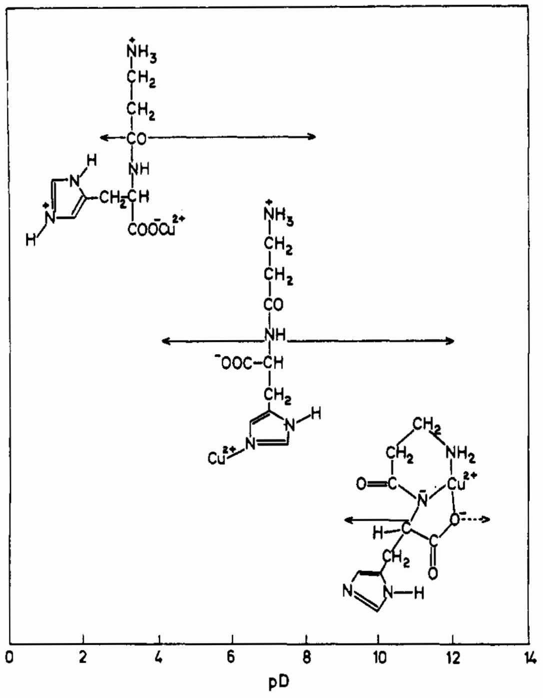

FIGURE 11: Distribution of complex species with pD. Approximate ranges of pD for the existence of the various complexes are indicated.

solution the copper binds to the carboxyl (Lenz and Martell, 1964), and the imidazole ring (Dobbie and Kermack, 1955; Martin and Edsall, 1960), and that the amino group and deprotonated peptide nitrogen become binding sites as the pD is increased. The main difference is that we observe binding to the N-3 nitrogen rather than the N-1 nitrogen of the imidazole ring whereas all previous authors concerned with solution studies agree that N-1 is the binding site. From his study of the binding of Mn^{2+} by carnosine at pH 7.65, Rosenberg (1961b) postulated one complex in which Mn^{2+} is bonded to the N-1 atom, with perhaps the carboxyl group also participating. The present results with Cu^{2+} are in line with his work *vis a vis* binding predominantly to imidazole at neutral pH, but again, in our case it is N-3 and not N-1.

Other differences in interpretation are also evident. Martin and Edsall (1960), concluded that in the pD region where both ionized amino and imidazole functions exist, Cu^{2+} is equally distributed between both. No concrete evidence for a complex in which the amino group is the sole ligand has been obtained in this work. All authors (Martin and Edsall, 1960; Martin, 1960; Lenz and Martell, 1964) agree with the suggestion of Dobbie and Kermack that the species in alkaline solution has simultaneous binding of Cu^{2+} to NH_2, N(peptide), and N-1. Our results are more in agreement with structure **3** resulting from the X-ray diffraction studies of Freeman and Szymanski (1965, 1967) in which the N-3 nitrogen is Cu^{2+} bonded except that we postulate a mixture of two species rather than one dimeric species as depicted.

References

Boas, J. F., Pilbrow, J. R., Hartzell, C. R., and Smith, T. D. (1969), *J. Chem. Soc. A*, 572.

Carrington, A., and McLachlan, A. D. (1967), Introduction to Magnetic Resonance, New York, N. Y., Harper & Row, p 228.

Dobbie, H., and Kermack, W. O. (1955), *Biochem. J. 59*, 246.

Edsall, J. T., Flory, P. J., Kendrew, J. C., Liquori, A. M., Nemethy, G., Ramachandran, G. N., and Scheraga, H. A. (1966), *J. Biol. Chem. 241*, 1004.

Freeman, H. C., and Szymanski, J. T. (1965), *Chem Commun.*, 598.

Freeman, H. C., and Szymanski, J. T. (1967), *Acta Crystallogr. 22*, 406.

Glasoe, P. K., and Long, F. A. (1960), *J. Phys. Chem. 64*, 188.

Hanson, H. T., and Smith, E. C. (1949), *J. Biol. Chem. 179*, 789.

Jungnickel, J. L. (1963), *Anal. Chem. 35*, 1985.

Kainosho, M. (1969), *J. Phys. Chem. 73*, 3516.

Lenz, G. R., and Martell, A. E. (1964), *Biochemistry 3*, 750.

Li, N. C., Scruggs, R. L., and Becker, E. D. (1962), *J. Amer. Chem. Soc. 84*, 4650.

Martin, R. B. (1960), *J. Amer. Chem. Soc. 82*, 6053.

Martin, R. B., and Edsall, J. T. (1960), *J. Amer. Chem. Soc. 82*, 1107.

Nakamura, A., and Jardetzky, O. (1968), *Biochemistry 7*, 1226.

Peisach, J., Aisen, P., and Blumberg, W. E., Ed. (1966), *in* The Biochemistry of Copper, Proceedings of an International Symposium, New York, N. Y., Academic.

Rosenberg, A. (1960a), *Arch. Biochem. Biophys. 88*, 83.

Rosenberg, A. (1960b), *Biochim. Biophys. Acta 45*, 297.

Rosenberg, A. (1961a), *Ark. Kemi 17*, 25.

Rosenberg, A. (1961b), *Ark. Kemi 17*, 41.

Sigel, H., Griesser, R., and McCormick, D. B. (1969), *Arch. Biochem. Biophys. 134*, 217.

Sternlicht, H., Shulman, R. G., and Anderson, E. W. (1965), *J. Chem. Phys. 43*, 3133.

Vallee, B. L. (1960), *Enzymes 3*, 225.

Williams, R. J. P. (1959), *Enzymes 1*, 391.